Man In India, 97 (4) : 1-11

CURRENT EXCURSION IN RELUCTANCE MACHINE USING CYCLIC INTEGRATION METHOD

Rajmal Joshi*, Dhansekaran R.** and Aravind C.V.***

Abstract: Torque generation in reluctance machines is based on the transition of mechanical motion of the rotor between aligned and unaligned position. As the rotor moves from unaligned to aligned, the inductance increases and the torque generated reduces. At aligned position, the torque generated is zero. Beyond aligned position as the rotor rotates from aligned to unaligned position a negative torque is generated. Hence, the need to remove current from the currently excited phase to the next phase is critical to ensure continuous positive torque generation. Since inductance is the function of rotor position it is important to understand the current excursion as the inductance varies in order for the controller to be effective, eventually reducing the torque ripple and the noise in the reluctance machines.

Index Terms: Inductance, current control, vibrations, rotor angle, stator.

INTRODUCTION

Electrical Machines are broadly classified as electro-magnetic (motion produced by the interaction of two magnetic fields) and variable reluctance (reluctance in the air gap between stator and rotor) based on the operating principle. Electro-magnetic based machines (in particular to induction motors & DC motors) are the work horse of the industry in the past decades even though their operating efficiency is not encouraging. Both the induction motor and DC motors drive able to be neither good for better dynamic performance nor for higher power density. In particular, with low rotation speeds or at standstill, both drive types have problems in producing satisfactory torques. Evolution of the modern semiconductor power switches and digital technology has opened up new opportunities in the development of sophisticated and tailor made electric drives for typical applications. The most modern machine drive systems today operate at high speeds, high mechanical torque at low speeds with simpler power devices. With the advancement in the powder metallurgy more new magnetic material leads to different configurations of electrical machines. The newer permanent magnet synchronous motors (PMSM) with surface mounted and interior permanent magnets are replacing the induction machines. Absence of rotor electrical circuit simplifies the analysis, but requires an absolute rotor position sensor in order to maintain the field orientation [1-2]. However Increase in annual usage of rare earth magnets has brought about the pricing up along with the magnet with high co-ercivity as the additives. For high torque density for small rated power applications a reluctance machines are

* Research Scholar, Department of EEE, Sathyabama University, Chennai

** Professor, Syed Ammal Engineering College, Ramanathapuram

*** School of Engineering, Taylor's Univesity Malaysia 47000

replacing the PMSM. As such is the doubly salient controlled reluctance machine (commercially known as Switched Reluctance Motor) utilising stepper motor reluctance principle (power range limited to a few hundred watts at maximum) to a power range of a few hundred kilowatts. A shaft-position encoder feedback is used along with the motor to synchronise the commutation of the phase currents for precise rotor position. As the name implies these machine cannot operate without the power electronic switches [3-12]. A SR drive system eradicates the commutation issues of the conventional universal current motors and at the same time gives better dynamic performance than an induction machine. These motors have quite simple constructions and their adjustable speed, current and torque features shows that this motor are really suitable for variable speed drive applications as in electric cars, elevators, centrifugal pumps[13-15] industrial transportation [16-17] and aerospace industry [6] [18-20]. SRM is used as generator in wind energy applications [21-23] and in automotive applications [24-25]. A linear SRM is used in Magnetic levitation [26] and more recently in high power density required applications, as in aircraft electric motor [27] using soft magnetic composites. A prototype machine with 6/4 poles is developed and experimentally tested. Figure 1 shows the developed SRM machine and the corresponding specification is shown in Table 1. This motor is analytically solved using the cyclic integration method and the proposed algorithm is tested for evaluations. An SRM with a 6/4-pole combination is considered for deriving the analytic procedure for the inductance evaluation.

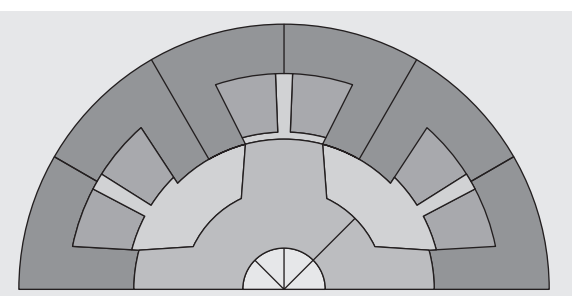

(a) Half section of a 6/4 SRM

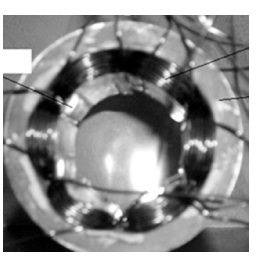

(a) Stator with coil

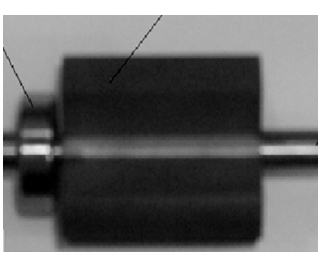

(b) Solid Rotor

Figure 1: Wheel slip response with the proposed control algorithm

TABLE 1: PROTOTYPE MACHINE DESIGN SPECIFICATIONS

Parameters	*Values*
Number of stator poles (P_s	6
Number of rotor poles	4
Stator pole arc	31
Rotor pole arc	33
Air gap length	0.1 mm
Bore Diameter	39 mm
Stack length	40 mm
Shaft diameter	0.3 mm
Stator back iron thickness	0.7 mm
Height of stator pole	10.8 mm
Height of rotor pole	9.7 mm
Turns per phase	110
Rated current	5
Lamination material	M19

CYCLIC INTEGRATION METHOD

(a) Cyclic Integration Method Algorithm

The cyclic integration method is based on taking all the flux lines in a stator pole face at once. This is done by considering a small portion of this face and taking into account its length and radius is integrated to get the inductance on the pole face. Two main assumptions are considered in this method namely:

1. The flux paths are concentric circles for any path longer than air gap.
2. The stator pole face is approximately flat within the interval of integration.

Based on these assumptions the integration method is performed to calculate the total reluctance of the stator pole face. Figure 2 shows the simple cross sectional section of the rotor stator interactions positions. This method starts with analysing the position of the rotor with respect to the excited stator winding. A small portion of the section is analytically computed to set as the initial computation point. The flux line as assumed in concentric, ends at the point of half pole pitch and is set as the end point. A permeance value is computed within this limit. From the permeance value the reluctance is computed through inverting the values. Now the value of the reluctance is integrated towards the longitudinal position of the rotor with respect to the stator (in this case of 4 rotor poles the end value is 360/4 which is 90°). This principle is repeated in the other side of the pole faces also. Once the full reluctance is computed the flux, inductance and the torque are calculated as in Equation (3)-(6).

The permeance (ΔP) of a small portion is computed as in Equation (1).

$$\Delta P = \frac{\mu l dr}{r d\theta} \tag{1}$$

where r is the radius of the region and l is the length of the region.

The permeance P_{radial} for an entire bounded region is then derived using the Equation (2).

$$P_{radial} = \int_{ll}^{ul} \frac{\mu l dr}{r d\theta} \tag{2}$$

where *ul* is the upper limit and *ll* is the lower limit.

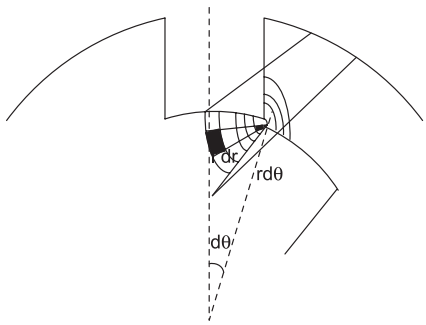

Figure 2: Cyclic integration method principles

The reluctance of the bounded region R_{radial} can then be calculated using Equation (3).

$$R_{radial} = \frac{1}{P_{radial}} \tag{3}$$

Total reluctance (R) of the stator pole face selected is calculated using Equation (4).

$$R = \int_{0}^{\pi/4} R_{radial} \tag{4}$$

The inductance is calculated for rotor positions in relation to the stator. For this method, the flux maps selected are for when the rotor positions are at fully unaligned position, fully aligned positions and intermediate positions such as that for partial conditions. From the reluctance is computed the flux (φ) is calculated and from the flux the torque of the machine under static condition is calculated using the Equation (5).

$$\varphi(\theta, i) = L(\theta, i)i \tag{5}$$

where θ and $L(\theta, i)$ are the rotor angular position and the phase inductance, respectively. Figure 3 shows the generalized inductance curve for various positions of the rotor. From the inductance characteristic the slope of the inductance is computed and the torque of the machine is calculated using Equation (6).

$$T = \frac{1}{2}\frac{dL}{d\theta} i^2 \omega \quad (6)$$

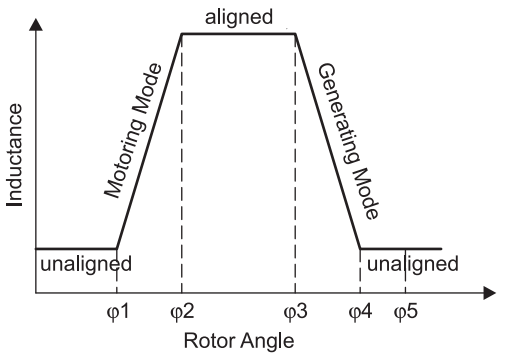

Figure 3: Inductance characteristics for various rotor positions

CURRENT EXCURSION COMPUTATIONS

(b) Unaligned Computations

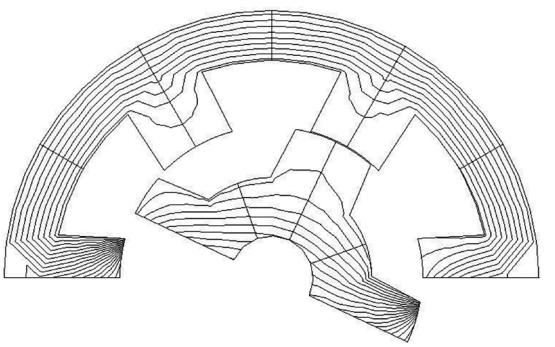

(a) Flux lines in unaligned conditions

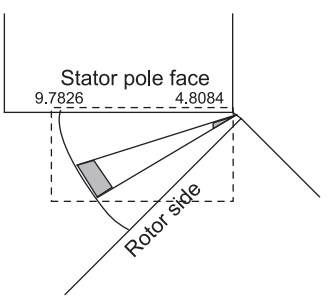

(b) Calculation limit under unaligned conditions

Figure 5: Unaligned calculations

Permeance of the small portion shaded grey

$$\Delta P = \frac{\mu l dr}{r d\theta} \tag{7}$$

Permeance of the entire flux path bounded for is given as

$$P_{radial} = \int_{4.8084}^{9.7826} \left(\frac{\mu l dr}{r d\theta} \right) \tag{8}$$

$$P_{radial} = \frac{\mu l (0.710241)}{d\theta} \tag{9}$$

$$R = \int_{0}^{\pi/4} \frac{d\theta}{\mu l (0.710241)} \tag{10}$$

$$L_2 = \frac{Tph \times \varnothing}{i} \tag{11}$$

(c) Aligned Computations

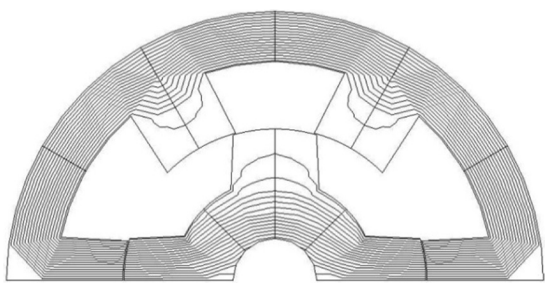

(a) Flux lines in aligned conditions

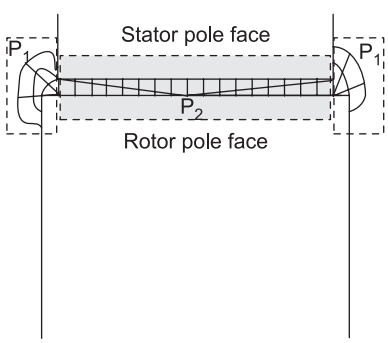

(b) Calculation limit under aligned conditions

Figure 6: Aligned calculations

Region 1: The limit of the angle is 0 to π while that of the radius is (coil clearance + air gap) = 0.6 mm to air gap = 0.1 mm

$$P_{radial} = \int_{0.1}^{0.6} \left(\frac{\mu l dr}{r d\theta} \right) \tag{12}$$

$$mmf = 2(L_{sp}H_{sp} + L_{sp}H_{sp}) + L_{sy}H_{sy} + L_{ry}H_{ry} + 2R\phi \tag{13}$$

$$R_{radial} = \frac{d\theta}{\mu l(1.79176)} \tag{14}$$

$$R = \int_{0}^{\pi} \frac{d\theta}{\mu l(dr)} \tag{15}$$

$$L_2 = \frac{Tph \times \varnothing}{i} \tag{16}$$

Region 2

$$R_g = \frac{lg}{\mu Ag} \tag{17}$$

$$A_g = \frac{A_{sp} + A_{rp}}{2} \tag{18}$$

(d) Intermediate Computations

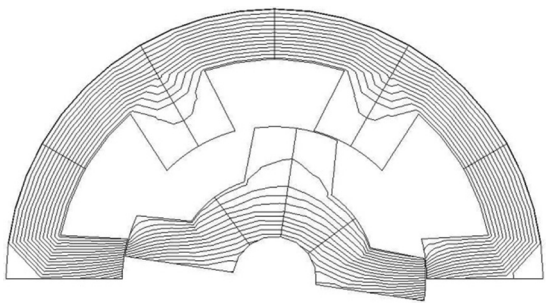

(a) Flux lines in intermediate conditions

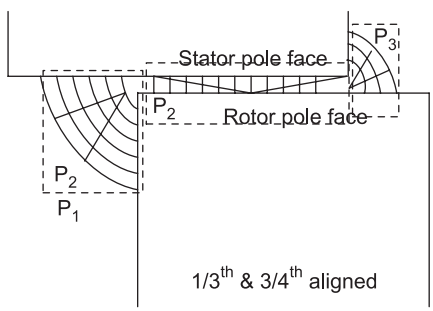

(b) Calculation limit under partial overlap conditions

Figure 7: Partial aligned calculations

Region 1: The limit of the angle is 0 to π while that of the radius is (coil clearance + air gap) = 0.6 mm to air gap = 0.1 mm

$$P_{radial} = \int_{0.1}^{5.078} \left(\frac{\mu l dr}{r d\theta} \right) = \frac{\mu l (3.9275)}{d\theta} \tag{20}$$

$$R_{radial} = \frac{1}{P_{radial}} = \frac{d\theta}{\mu l (3.9275)} \tag{21}$$

$$R = \int_{0}^{1.3003} \frac{d\theta}{\mu l (3.9275)} \tag{22}$$

Region 2:

$$P_{radial} = \frac{lg}{\mu Ag} \tag{23}$$

Region 3:

$$P_{radial} = \int_{0.1}^{0.6} \left(\frac{\mu l dr}{r d\theta} \right) = \frac{\mu l (1.79176)}{d\theta} \tag{24}$$

$$R_{radial} = \frac{1}{P_{radial}} = \frac{d\theta}{\mu l (1.79176)} \tag{25}$$

$$R = \int_{0}^{\pi/2} \frac{d\theta}{\mu l (1.79176)} \tag{26}$$

Region 1: The limit of the angle is 0 to π while that of the radius is (coil clearance + air gap) = 0.6 mm to air gap = 0.1 mm

$$P_{radial} = \int_{0.1}^{0.6} \left(\frac{\mu l dr}{r d\theta} \right) \tag{27}$$

RESULTS AND DISCUSSIONS

Table 2 shows the computations of the inductance values at various positions using the cyclic integration method. In the intermediate position the flux lines are divided into several flux lines and is used for the analysis of the machines.

TABLE 2: INDUCTANCE VALUES AT VARIOUS POSITIONS

Position	*Inductance Value (mH)*
0	1.3443
10	1.1299
20	4.2734
30	8.6633
40	13.097

Position	*Inductance Value (mH)*
50	16.233
60	13.097
70	8.663
80	4.2734
90	1.1299

TABLE 3: COMPARATIVE EVALUATIONS

	Experimental	*FEA*	*CIM*
Unaligned (mH)	1.3443	1.1	1.4518
Aligned (mH)	16.3	14.6	15.39
Slope	0.023	0.025	0.0239
Average Torque (Nm)	0.287	0.28	0.299

TABLES, FIGURES, EQUATIONS

CONCLUSION

Cyclic Integration method for computing the current extrusion through the inductance is introduced and is used to anlayse for the prototyped machine. Comparison of the experimental design under laboratory environment is compared with that of the proposed method. Also using FEA tool the machine is analysed to confirm the effectiveness of the proposed method. Since in reluctance machine there is no secondary energy source is involved the computations are relatively simpler compared to that of the dual energy excited systems.

Acknowledgment

Authors acknowledge research students Samuel Bright and Grace Ikujani for performing the simulation of the design.

References

Thomas M.J, Gerald B.K. and Thomas W.N. (1986). “Interior Permanent-Magnet Synchronous Motors for Adjustable-Speed Drives”. IEEE Transactions on Industry Applications, Vol. 1A-22, No. 4, July/Aug 1986. pp. 738-747.

Dan N. Lonel. (2008). “IPM Motors : A Solution for High Performance Appliances” Appliance Magazine. Nov. 2008.

P.J. Lawrenson, J.M. Stephenson, J. Corda, and N.N. Fulton, IEE Proceedings B 127, 253 (1980).

T.E.J. Miller, and M. McGill, IEE Proceedings B 137, 337 (1990).

J. Faiz, and J.W. Finch, IEEE Trans. on Energy Conversion 8, 704 (1993). 783

T.J.E. Miller, Switched Reluctance Motors and Their Control (Oxford University Press, 1993).

D.A. Torrey, X-M. Niu, and E.J. Unkauf, IEE Proceedings Electric Power Application 142, 14 (1995).

A.V. Radun, IEEE Trans. on Industry Applications 31, 1079 (1995).

S. Brisset, and P. Brochet, IEEE Trans. on Magnetics 34, 2853 (1995).

I. Boldea and S.A. Nasar, Electric Drives, Ch. 12 (CRC Press, 1999).

C. Roux, and M.M. Morcos, IEEE Trans. on Energy Conversion 17, 400 (2002).

Lim H.S, R. Krishnan and N.S. Lobo Design and Control of a linear propulsion system for an elevator using linear switched reluctance motor drives IEEE Trans. Ind. Elect., 55:535-542 (2008)

Cheng-Tsung Liu, Yan-Nan Chen, Ming-Huei Lee, Yue-Jen Lee, 'Operational Characteristics of a Zero-Torque Linear Switched-Reluctance Machine for Magnetic Levitation and Propulsion System', Conference Digest of INTERMAG '97, 35th IEEE International Magnetics Conference, New Orleans, LA, USA, 1-4 April, 1997, Paper BR-08.

El-Khazendar, 'A Battery-supplied traction drive for electric vehicles', Proceedings of ICEM '94, International Conference on Electrical Machines, Paris, France, 5-8 September, 1994, Vol. 1, pp. 226-231.

K.H. Rahman, B. Fahimi, G. Uresh, A.V. Raharathnam, M. Ehsani, 'Advantages of Switched Reluctance Motor Application to EV and HEV: Design and Control Issues', Conference Record of IAS '98, the 1998 IEEE Industry Applications Society 33rd Annual Meeting, St.

Louis, MO, USA, 12-15 October, 1998, Vol. 1, pp. 327-334.

J.M. Miller, A.R. Gale, P.J. McCleer, F. Leonardi, J.H. Lang, 'Starter-Alternator for Hybrid Electric Vehicle: Comparison of Induction and Variable Reluctance Machines and Drives', Conference Record of IAS '98, the 1998 IEEE Industry Applications Society 33rd Annual

Meeting, St. Louis, MO, USA, 12-15 October, 1998, Vol. 1, pp. 513-524.

"Green Technologies for the Energy-optimized Clouds" in Asian Journal of Research in Social Sciences and Humanities, Vol. 6, Issue 6, Special Issue June 2016.

L. Chang, 'Control of a Switched Reluctance Motor for Automotive Applications', Proceedings of CCECE '98, 11th IEEE Canadian Conference on Electrical and Computer Engineering, Waterloo, ON, Canada, 24-28 May, 1998, Vol. 1, pp. 393-396.

S.K. Mondal, S.N. Bhadra, S.N. Saxena, 'Application of current-source converter for use of SRM Drive in transportation area', Proceedings of PEDS '97, the 2nd IEEE International Conference on Power Electronics and Drive Systems, Singapore, 26-29 May, 1997, Vol. 2, pp. 708-713.

"Public Control Algorithm for a Multi Access Scenario comparsing GPRS and UMTS ",at Department of Computer Science and Engineering, National Conference on "Intelligent computing With IoT on April 16 2016 in Dhirajlal Gandhi College of Technology.

D.A. Torrey, S.E. Childs, S de Haan, 'A Variable-Speed Wind Turbine Based on a Direct-Drive Variable-Reluctance Generator', Proceedings of Windpower '94, Minneapolis, MN, USA, May, 1994, pp. 513-522.

I. Haouara, A. Tounzi, F. Piriou, ' Study of a Variable Reluctance Generator for Wind Power Conversion', Proceedings of EPE '97, 7th European Conference on Power Electronics and Applications, Trondheim, Norway, 8-10 September, 1997, Vol. 2, pp. 631-636.

R. Cardenas, W.F. Ray, G.M. Asher, 'Switched Reluctance Generators for wind Energy Applications', PESC '95 Record. 26th Annual IEEE Power Electronics Specialists Conference, Atlanta, USA, 18-22 June, 1995, Vol. 1, pp. 559-564.

H.M.B. Metwally, W.R. Anis, 'Performance Analysis of PV Pumping Systems using Switched Reluctance Motor Drives', Energ. Convers. Mgmt, vol. 38, no.1 pp. 1-11, 997, Elsiever Science Ltd, ISBN 0196-8904/97.

C.A. Ferreira, S.R. Jones, B.T. Drager, W.S. Heglund, 'Design and Implementation of a Five Horsepower, Switched Reluctance Fuel-Lube, Pump Motor Drive for a Gas Turbine Engine', IEEE Transactions on Power Electronics, Vol. 10, No. 1, January, 1995, pp. 55-61.

T.L. Skvarenina, S. Pekarek, O. Wasynczuk, P.C. Krause, 'Simulation of Switched Reluctance, More Electric Aircraft Power System using a Graphical User Interface', Proceedings of IECEC '96, IEEE 31st Intersociety Energy Conversion Engineering Conference, 11-16 August, 1996, Vol. 1, pp. 143-147.